A nucleotide substitution model with nearest-neighbour interactions

Gerton Lunter and Jotun Hein

Bioinformatics group, Dept. of Statistics, Univ. of Oxford,
1 South Parks Road, Oxford OX1 3TG, U.K.
Telephone +44 1865 285366, Fax +44 1865 272595

ABSTRACT

Motivation: It is well known that neighbouring nucleotides in DNA sequences do not mutate independently of each other. In this paper, we introduce a context-dependent substitution model and derive an algorithm to calculate the likelihood of sequences evolving under this model. We use this algorithm to estimate neighbour-dependent substitution rates, as well as rates for dinucleotide substitutions, using a Bayesian sampling procedure. The model is irreversible, giving an arrow to time, and allowing the position of the root between a pair of sequences to be inferred without using outgroups.

Results: We applied the model on aligned human-mouse noncoding data. Clear neighbour dependencies were observed, including $17 - 18$ fold increased CpG to TpG/CpA rates compared to other substitutions. Root inference positioned the root halfway the mouse and human tips, suggesting an approximately clock-like behaviour of the irreversible part of the subsitution process.

Contact: lunter@stats.ox.ac.uk

INTRODUCTION

Most current stochastic models for the evolutionary nucleotide substitution process in DNA sequences assume that neighbouring sites evolve independently. This considerably simplifies calculations, since under this assumption, the likelihood is the product of individual site likelihoods. However, there is ample evidence that independence is violated (Karlin and Burge (1995)), for example by the well-known methylation-induced rate increase of C to T (and G to A) substitutions in vertebrate CpG dinucleotides. The importance of neighbour dependencies in the substitution process has long been recognised, and several ways of modelling these dependencies have been proposed. For example, Siepel and Haussler (2003) show that a Markov chain along a pair of sequences fits sequence data substantially better than a series of independent pairwise nucleotide distributions (a "zeroth-order" Markov chain) do.

A natural model for context-dependent substitutions is one which assigns rates to every possible dinucleotide-to-dinucleotide substitution, which then apply to all overlapping neighbouring nucleotide pairs in a sequence. This model,

referred to as the "dinucleotide model", is arguably the simplest possible general evolutionary model that takes neighbour dependencies into account, and captures (neighbour independent) dinucleotide substitutions as well. One of its essential features is that long-range dependencies between sites immediately arise, due to the possibility of overlapping hits. Because of this 'contagious dependence', this model is harder to analyse than independent-site models. Previous studies by Jensen and Pedersen (2000) and Arndt et al. (2003) used similar explicit evolutionary models, both in the nucleotide and codon contexts, and focussed primarily on the relation between the rate matrix and the equilibrium sequence distribution. As the equilibrium distribution contains only partial information on the substitution rates, this can be used only for estimation of sparsely parameterised models. For richer models it is necessary to have a method for calculating the likelihood of observing a pair of homologous sequences. Pedersen and Jensen (2001) developed an MCMC approach for a codon model with neighbour dependencies to estimate this likelihood. Their method involves no approximations, but does require potentially long sampling runs for reliable likelihood estimates, making it less suitable for parameter inference. Another method was introduced by Whelan and Goldman (2004), who use a 'mean field' approach to recover site independence, and use this to infer dinucleotide substitution rates in a codon model. von Haeseler and Schöninger (1998) use a reversible model based on observed nucleotide (or amino acid) doublet frequencies, and estimate the expected number of mutations as a function of Hamming distance using MCMC. The recent paper by Siepel and Haussler (2004) is perhaps closest in its aims to the present paper. They use a Markov model on a phylogenetic tree, parameterized by a dinucleotide rate matrix and an independent-site equilibrium sequence distribution, and estimate substitution parameters using an EM procedure.

In this paper we present a fast, analytic method for calculating the joint likelihood of observing two homologous sequences evolving under the dinucleotide model. This makes it possible to infer parameter, either by maximum likelihood, or in a Bayesian fashion. Our approach has the advantage of
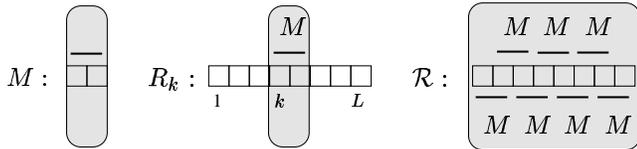
Fig. 1. Illustration of the dinucleotide model. Horizontal bars indicate instantaneous (rate) dependencies, grey areas indicate regions of finite-time dependencies due to 'contagious dependence'. The model is parameterized by a 16×16 matrix M, specifying mutation rates on dinucleotides. The matrix R_k has dimension $4^L \times 4^L$, and corresponds to M acting on nucleotides k and $k+1$ only, with no mutation process acting on any other nucleotides. Formally, it is the 'matrix concatenation sum' of the null matrix acting on the leftmost $k-1$ nucleotides, the matrix M, and the null matrix acting on the remaining $L-k-1$ nucleotides (see Appendix). The full model has rate matrix $\mathcal{R} = \sum_{k=1}^{L-1} R_k$, corresponding to the dinucleotide substitution process acting on all $L-1$ dinucleotides simultaneously.

using an explicit evolutionary ("process-based") model, and takes into account the equilibrium sequence distribution as a function of the substitution rate parameters. We demonstrate the method by estimating substitution rates and confidence intervals on noncoding human-mouse data. The algorithms involve some approximations, and we show by experiments on synthetic data that mutation rates can be faithfully recovered, using a Bayesian MCMC sampling approach, in the parameter range corresponding to that of human-mouse data.

In contrast to most stochastic models used in evolutionary biology, the proposed model is naturally irreversible. Reversible models enjoy technical advantages, for instance, they have roughly half as many parameters as irreversible models, and have symmetry properties that are helpful for deriving properties of such models, and in practical computations. For example, Felsenstein (1981) coined the Pulley Principle, which states that the likelihood of sequences evolving according to a reversible substitution model on a phylogenetic tree is independent of the position of the root, so that root placement is only possible using an outgroup as reference. However, there is no a-priori reason to assume reversibility, since many biological processes have a distinct direction in time, and this is certainly true for evolutionary processes. The possibility of rooting trees under irreversibile models of substitution was noted before, see e.g. Yang (1994), but for single nucleotide models the signal seems to be weak, especially in non-coding DNA (data not shown). The proposed dinucleotide model incorporates the profoundly directional CpG effect, making the model strongly irreversible, and we show that it is possible to infer root positions, even for just two sequences.

The paper is organized as follows. First we introduce the model, and discuss some of its properties. We then use Bayesian MCMC sampling to infer the model parameters. First, the method is validated by inferring parameters from synthetic data. The same procedure is then used on two sets

of 100 kb non-coding human-mouse aligned sequence data from human chromosomes 21 and 10. A discussion concludes the paper. Finally, in the Appendix we formally define the proposed model, and derive the algorithms for computing the equilibrium distribution, the sequence-to-sequence likelihood, and the likelihood that two sequences have evolved from an unknown common ancestor.

THE DINUCLEOTIDE SUBSTITUTION MODEL

We now introduce the 'dinucleotide model', a continuous-time Markov model for nucleotide substitutions. The parameters of the model are given by a 16×16 rate matrix M, whose rows and columns are labelled by the 16 possible nucleotide pairs, so that the matrix describes mutation rates from any nucleotide pair to any other. These rates apply to each of the $L-1$ pairs of neighbouring nucleotides in a sequence of length L simultaneously (see Fig. 1). The rate matrix of the full model, denoted by $\mathcal{R}$, specifies rates at which any length-L *sequence* mutates into any other. This matrix has has dimension $4^L \times 4^L$, but is very sparse; in fact $R_{\sigma,\tau}$, the rate at which sequence σ mutates into τ, vanishes unless σ and τ coincide apart from at most two consecutive nucleotides.

The dinucleotide substitution model introduces dependencies between neighbouring sites, and the stationary sequence distribution $\pi(\sigma)$ no longer factorises into a product of single-nucleotide distributions as in the independent-site model (see Appendix for an algorithm to compute the stationary distribution). The relation between the parameters of the model (the
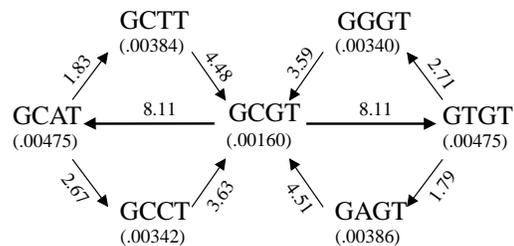

Fig. 2. Example of irreversibility in the dinucleotide model. Depicted is part of the full Markov chain for sequences of length 4. In this example, rates for the mutation of CG into TG or CA are both 1.0 mutations per observed pair and per time unit, while every other neighbour-dependent mononucleotide substitution occurs with rate 0.1. The resulting equilibrium probabilities for the length-4 sequences are shown between brackets (see Appendix), and equilibrium flows (in units of 10^{-4} transitions per unit of time) are shown alongside the arrows, which point in the direction of net flow. Two rate parameters contribute to each single nucleotide substitution rate, e.g. both CG → TG and GC → GT contribute to the GCGT → GTGT transition, so that the net flow at equilibrium along the edge GCGT–GTGT is $.00160 \times (1.0 + 0.1) - .00475 \times (0.1 + 0.1) = .00081$. This violation of "detailed balance" implies irreversibility; for example, the cycle GCGT → GTGT → GGGT → GCGT is more likely to occur than its reversal, giving a definite direction to time.

(a)

	A				C				G				T			
	A	C	G	T	A	C	G	T	A	C	G	T	A	C	G	T
A	*	$.077^9$	$.080^9$	$.084^9$	*	$.076^8$	$.067^6$	$.068^7$	*	$.076^9$	$.092^9$	$.069^8$	*	$.072^7$	$.074^8$	$.082^7$
C	$.081^9$	*	$.074^8$	$.069^6$	$.069^6$	*	$.08^1$	$.08^1$	$.17^6$	*	$.13^5$	2.47^9	$.08^1$	*	$.078^9$	$.08^1$
G	$.069^6$	$.080^9$	*	$.073^7$	$.076^9$	$.076^9$	*	$.08^1$	$.077^8$	$.076^9$	*	$.072^8$	$.085^8$	$.073^8$	*	$.075^8$
T	$.077^9$	$.074^9$	$.081^8$	*	$.09^1$	$.069^8$	$.09^1$	*	$.081^8$	$.09^1$	$.067^4$	*	$.065^5$	$.077^9$	$.081^9$	*

$\rho_1 = 0.509 \pm 0.007$ (true 0.502)

$\rho_2 = 0.018 \pm 0.003$ (true 0.020)

(b)

	A				C				G				T			
	A	C	G	T	A	C	G	T	A	C	G	T	A	C	G	T
A	*	$.031^6$	$.054^4$	$.008^2$	*	$.028^5$	$.18^1$	$.041^7$	*	$.060^9$	$.16^1$	$.066^8$	*	$.06^1$	$.16^1$	$.034^8$
C	$.05^1$	*	$.024^6$	$.14^1$	$.04^1$	*	$.018^3$	$.29^1$	$.11^7$	*	$.09^4$	2.55^{12}	$.011^7$	*	$.030^8$	$.076^8$
G	$.19^1$	$.052^9$	*	$.05^1$	$.11^1$	$.073^9$	*	$.06^1$	$.076^8$	$.018^3$	*	$.010^7$	$.24^2$	$.07^1$	*	$.07^1$
T	$.058^7$	$.14^1$	$.040^9$	*	$.009^3$	$.054^4$	$.026^3$	*	$.011^5$	$.12^1$	$.049^8$	*	$.029^7$	$.14^1$	$.030^5$	*

$\rho_1 = 0.469 \pm 0.005$

$\rho_2 = 0.016 \pm 0.002$

(c)

	A				C				G				T			
	A	C	G	T	A	C	G	T	A	C	G	T	A	C	G	T
A	*	$.029^3$	$.055^4$	$.019^2$	*	$.032^5$	$.19^1$	$.022^4$	*	$.033^5$	$.151^9$	$.049^8$	*	$.067^8$	$.12^1$	$.026^5$
C	$.073^9$	*	$.021^5$	$.046^6$	$.06^1$	*	$.018^3$	$.27^1$	$.30^6$	*	$.26^6$	2.30^{10}	$.004^3$	*	$.022^5$	$.07^1$
G	$.19^1$	$.044^7$	*	$.052^7$	$.16^1$	$.059^7$	*	$.03^1$	$.045^5$	$.017^2$	*	$.004^3$	$.25^1$	$.071^8$	*	$.04^1$
T	$.025^5$	$.18^1$	$.030^3$	*	$.019^2$	$.055^4$	$.029^3$	*	$.023^6$	$.19^1$	$.041^8$	*	$.025^5$	$.132^8$	$.031^4$	*

$\rho_1 = 0.457 \pm 0.005$

$\rho_2 = 0.015 \pm 0.002$

Fig. 3. Estimated mononucleotide substitution rates (dependent on unchanged right neighbour [top row]; left-neighbour dependent rates are fixed by strand reversal symmetry), total mononucleotide rate (ρ_1) and total dinucleotide rate (ρ_2). Superscripts indicate one standard deviation in the last digit(s). **(a)** Synthetic data; true mononucleotide rates: CG $\rightarrow$ TG, 2.40; all others, 0.075. **(b)** Chromosome 21 and **(c)** 10.

coefficients of M) and the reversibility of $\mathcal{R}$ is more complicated than for independent-nucleotide models, as it involves this equilibrium sequence distribution. Even for a reversible M (on length-2 sequences), the total matrix $\mathcal{R}$ is in general irreversible. For example, M may specify detailed balance for CG $\leftrightarrow$ TG state transitions if confined to length-2 sequences, but state transitions of longer sequences that involve mutations overlapping the C or G residue may disrupt detailed balance by creating additional CG dinucleotides, leading to cycles in the equilibrium flow graph (see Fig. 2).

The matrix $\mathcal{R}$ is far too big to use explicitly. It turns out that it is possible to compute $\exp(\mathcal{R}t)_{\sigma,\tau}$, the probability that sequence σ evolves into τ in time t, without computing the matrix exponential explicitly, through a dynamic programming recursion that uses the structure of $\mathcal{R}$. Exact results still involve large matrices, and approximations are necessary. Our approximation consists of ignoring all terms related to multiple substitutions involving 4 or more consecutive nucleotides. Such events comprise at least 3 independent 'overlapping' substitutions, so that the leading error term is cubic in the divergence time and mutation rate. To validate the approximation in the parameter range of interest, we do parameter inference on synthetic data.

EVALUATION AND RESULTS

For the substitution model, we used only a subset of the 240 free parameters in the matrix M. The symmetry of the substitution process under reverse-complement means that all mononucleotide substitutions can be described by the $4 \times 4 \times 3 = 48$ right-neighbour rates only. General dinucleotide substitutions would require another 80 parameters, but since such substitutions are rare, reliable parameter inference requires much input data, and for this reason we use a single dinucleotide substitution rate parameter, 49 parameters in all.

Synthetic sequence data was produced by simulating the dinucleotide substitution model on a 100 kb sequence. We chose parameters to roughly mimic the parameters expected for human-mouse data, namely, a mononucleotide substitution rate of 0.075 for all substitutions except CG $\rightarrow$ TG (and CA) which occur with rate 2.4. Summing over the implied equilibrium sequence distribution yields a total mononucleotide substitution rate of 0.502 substitutions per site and unit of time. We chose a total dinucleotide substitution rate of 0.020 dinucleotide substitutions per site and unit of time. Since about half as many substitutions have occurred in humans compared to mice since divergence (E. S. Lander *et al.* (2002)), we chose the root position to be 0.3 time units from the "human" descendant, and 0.7 units from the "mouse" sequence.

Neutrally evolving aligned human-mouse sequence data was prepared from BlastZ-aligned data (ftp://genome.ucsc.edu/-goldenPath/10april2003/vsMm3/axtBest/). We applied a simple but stringent syntheny filter to remove any spurious hits, then removed alignments that overlapped with genes (including introns and regulatory elements), that included repeats (both transposons and tandem repeats), or for which the DUST program (cutoff 16) annotated part of the alignment as a low entropy region. We further removed CpG islands (defined as 250 bp windows containing in excess of 7.5% CpGs, including their 125 bp shoulders; this removed 1.0% of sequence).
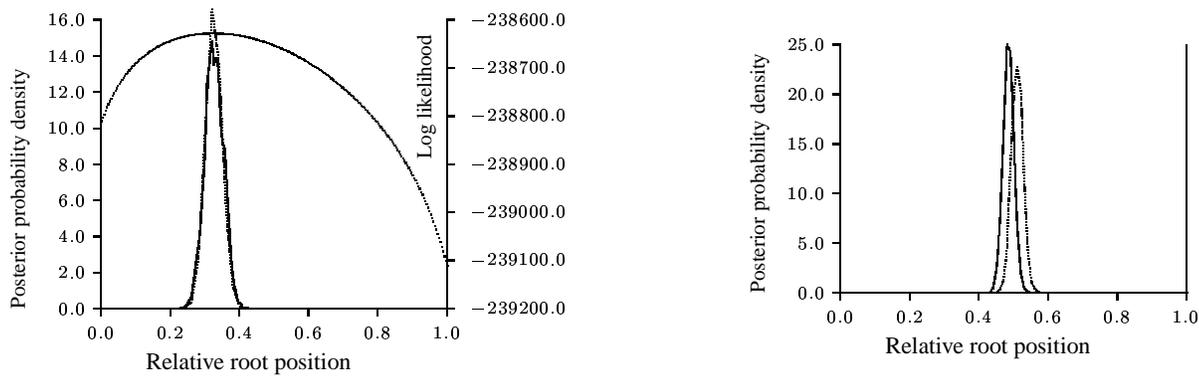
Fig. 4. Posterior density estimates of the root position. **Left:** Results for synthetic data. The theoretical posterior (with rate matrix fixed to correct values) is shown for comparison (dotted line); the smooth curve is the log likelihood. The sampled posterior is slightly broadened, due to the co-sampling of rates together with the root position parameter. **Right:** Results for chromosomes 21 (solid line) and 10 (dotted line).

The remaining data was cut up into individual ungapped alignments. Since there is evidence that sequences shorter than about 12 nucleotides cannot always be aligned correctly (data not shown), we trimmed the alignments by removing the leading and trailing 12 nucleotides, and subsequently removed alignments of less than 10 bases. Finally, we randomly selected a $\approx$ 100 kb subset of the resulting alignments. This procedure was carried out for human chromosome 21 (101142 nt) and chromosome 10 (99563 nt).

Results

Parameter estimation was done by Bayesian MCMC sampling running for 600.000 iterations, using flat priors for all parameters. Estimated sample sizes were good at 300–500 for the log likelihood, and typically 100 for the various matrix entries.

The rate estimates from synthetic data are shown in Fig. 3**a**. The estimated total mono– and dinucleotide rates are within one standard deviation of their true values. This is also true for over 80% of the matrix entries, including the $CG \rightarrow TG$ rate parameter, suggesting that the estimation method is unbiased. The $CG \rightarrow AG$ and $CG \rightarrow GG$ rates come out high, probably due to a combination of crosstalk from the high $CG \rightarrow TG$ rate and the three-site approximation we use; with a lower $CG \rightarrow TG$ rate no bias was observed (data not shown). The estimated posterior density for the root position is shown in Fig. 4**a**. The true root position is within one standard deviation of the Bayesian estimate of 0.33 ± 0.03.

Rate estimates based on human chromosome 21 (C21) and chromosome 10 (C10) data are shown in Fig. 3**b** and **c**. The estimates for the two chromosomes are broadly similar. The $CG \rightarrow TG$ rates are higher than the average mononucleotide rates by a factor 18 (C21; CpG abundance 0.93%) and 17 (C10; CpG abundance 1.06%). The total effective substitution rate for C21, due to mononucleotide and dinucleotide substitutions, is $0.469 + 2 \times 0.016 = 0.501$. Of this, $9.4 \pm 0.5\%$ is due to the CpG effect, and a further $6.4 \pm 0.8\%$ is due to dinucleotide substitutions. For C10,the total rate is 0.487, of

which $10.0 \pm 0.5\%$ is due to the CpG effect, and $6.2 \pm 0.8\%$ to dinucleotide substitutions.

Root positions for chromosome 21 and 10 were estimated at 0.484 ± 0.014 and 0.510 ± 0.016 respectively. Fig. 4**b** plots the posterior densities for both chromosomes.

Fig. 5 gives a reparametrised view of the rate estimates, obtained by separating out the neighbour-independent and neighbour-dependent substitution rates. For the synthetic data, the latter are theoretically zero, but since rates are nonnegative, they have a non-Gaussian distribution with nonzero mean. We used this parametrisation to test neighbour dependence, by using synthetic data to estimate cutoff values for the neighbour independent rates relative to their empirical standard deviation. A cutoff of 2.2 empirical standard deviations was found to correspond to a 90% confidence level. As expected, the hypothesis of neighbour independence can be rejected for the $CG \rightarrow TG$ substitution, and indeed for many more.

Discussion

We have introduced a context-dependent substitution model, that enables direct estimates of neighbour-dependent and dinucleotide substitution rates. The model is furthermore time-irreversible, which allows root placement in the absence of an outgroup.

We found strong $CG \rightarrow TG$ and CA substitution rates as expected, 17 and 18 times above the average rate for other dinucleotides, in agreement with previous estimates of a 10–20 fold increase (Sved and Bird (1990)). Our results indicate that the CpG-related substitutions accounts for about 10% of all substitutions, while an estimate by Subramanian and Kumar (2003) puts the CpG contribution to point substitutions in primate intergenic DNA to $\sim 20\%$. This twofold difference may be partly explained by a different balance of ordinary vs. CpG mutations in primates compared to rodents. In concordance with this hypothesis, we find a lower incidence of CpGs in our human chromosome 21 dataset compared to mouse, although in chromosome 10, the proportions are similar.
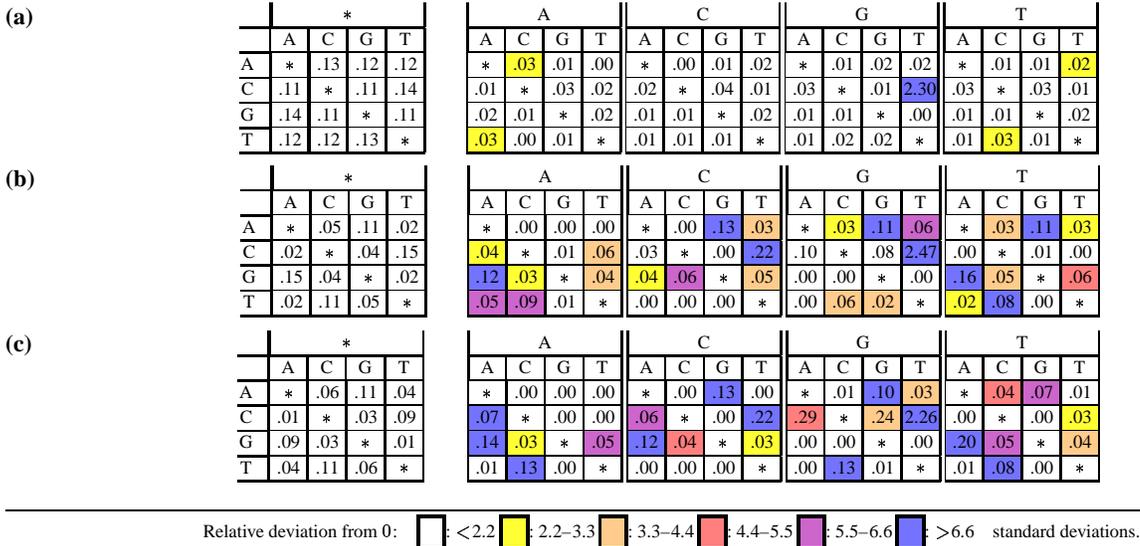
(a)

	*				A				C				G				T			
	A	C	G	T	A	C	G	T	A	C	G	T	A	C	G	T	A	C	G	T
A	*	.13	.12	.12	*	.03	.01	.00	*	.00	.01	.02	*	.01	.02	.02	*	.01	.01	.02
C	.11	*	.11	.14	.01	*	.03	.02	.02	*	.04	.01	.03	*	.01	2.30	.03	*	.03	.01
G	.14	.11	*	.11	.02	.01	*	.02	.01	.01	*	.02	.01	.01	*	.00	.01	.01	*	.02
T	.12	.12	.13	*	.03	.00	.01	*	.01	.01	.01	*	.01	.02	.02	*	.01	.03	.01	*

(b)

	*				A				C				G				T			
	A	C	G	T	A	C	G	T	A	C	G	T	A	C	G	T	A	C	G	T
A	*	.05	.11	.02	*	.00	.00	.00	*	.00	.13	.03	*	.03	.11	.06	*	.03	.11	.03
C	.02	*	.04	.15	.04	*	.01	.06	.03	*	.00	.22	.10	*	.08	2.47	.00	*	.01	.00
G	.15	.04	*	.02	.12	.03	*	.04	.04	.06	*	.05	.00	.00	*	.00	.16	.05	*	.06
T	.02	.11	.05	*	.05	.09	.01	*	.00	.00	.00	*	.00	.06	.02	*	.02	.08	.00	*

(c)

	*				A				C				G				T			
	A	C	G	T	A	C	G	T	A	C	G	T	A	C	G	T	A	C	G	T
A	*	.06	.11	.04	*	.00	.00	.00	*	.00	.13	.00	*	.01	.10	.03	*	.04	.07	.01
C	.01	*	.03	.09	.07	*	.00	.00	.06	*	.00	.22	.29	*	.24	2.26	.00	*	.00	.03
G	.09	.03	*	.01	.14	.03	*	.05	.12	.04	*	.03	.00	.00	*	.00	.20	.05	*	.04
T	.04	.11	.06	*	.01	.13	.00	*	.00	.00	.00	*	.00	.13	.01	*	.01	.08	.00	*

Relative deviation from 0:   : < 2.2 : 2.2–3.3 : 3.3–4.4 : 4.4–5.5 : 5.5–6.6 : > 6.6 standard deviations.

Fig. 5. Testing neighbour dependence of mononucleotide substitutions. The first matrix tabulates the neighbour-independent contribution to the substitution rates (row, original; column, mutant), the other four tabulate rates depending on the (unchanged) right neighbour (indicated at top). For each of these rates, the sample average was compared to the estimated standard deviation to indicate the confidence level at which the zero-rate hypothesis can be rejected (indicated by colors; white corresponds to a 90% level threshold as calibrated on synthetic data). **(a)** Synthetic data. Only the CG $\rightarrow$ TG rate is significantly non-zero, as expected. **(b)** Results for chromosome 21 and **(c)** chromosome 10.

The inferred relative contribution of dinucleotide substitutions to the overall per-site substitution rate of about 6% in presumably neutrally evolving human-mouse DNA is in broad agreement to a study by Averof et al. (2000), who reported a figure equivalent to 4%. However, Smith et al. (2003) convincingly argued that this estimate could be upwardly biased by rate variation along the genome, an effect we did not include, but is known to be important. A partial filtering for such rate variation resulted in a twofold reduction in the dinucleotide rate estimates (data not shown), suggesting that the figure of 6% is an overestimate.

The inferred root position is almost halfway the human and mouse tips. This is surprising since the mouse lineage has attracted about twice as many point mutations as the human lineage since divergence (E. S. Lander *et al.* (2002)). Since the root inference is based solely on the irreversible signal in the data, one possible explanation is that the mutation processes in mouse and human are not identical, even after scaling, but are a combination of an evolutionarily relatively constant irreversible process and a scaled reversible process reponsible for the majority of observed mutations. This hypothesis can be tested by inferring substitution rates on both lineages independently, using ancestral repeats.

The dinucleotide model will hopefully contribute to more precise phylogenetic estimates, by the ability of root inference, and its more accurate modelling of the neutral substitution process. We also intend to use it for a more accurate estimate of the proportion of the human genome under purifying selection, which is currently estimated at 5% (E. S. Lander *et al.* (2002)). Finally, it may find application in the evolutionary modelling of RNA base stacking, where context dependencies are known to be important.

Acknowledgements

APPENDIX

Formal definition of the model

To describe the model more formally, we introduce some notation. Let $\Omega = \{A, C, G, T\}$ be the alphabet, and Ω^L the state space of sequences. The space of probability distributions over Ω^L is denoted by $\mathcal{D}_L \subset \mathbf{R}^{4^L}$, and a probability distribution $v \in \mathcal{D}_L$ is a vector assigning a probability to all 4^L possible sequences in Ω^L. We label the coordinates of $\mathcal{D}_L$ by sequences, so that if $v \in \mathcal{D}_L$ and $\sigma \in \Omega^L$, v_σ is the probability of observing the sequence σ. Similarly, for a matrix A, a matrix coefficient is written $A_{\sigma, \tau}$, and is interpreted as the rate at which sequence σ mutates into τ (for rate matrices), or the probability that sequence σ mutates into τ (for probability matrices). We write $\sigma\tau$ for the concatenation of σ and τ, and we write $\sigma[i, j]$ for the subsequence $\sigma_i \sigma_{i+1} \cdots \sigma_j$. For rate matrices A, B acting on $\mathcal{D}_k$ and $\mathcal{D}_l$ respectively, we denote by $A \oplus B$ (the *matrix concatenation sum* of A and B) the

matrix acting on $\mathcal{D}_{k+l}$ that has A acting on the leftmost k residues of the sequence, so that it does not depend on nor changes the rightmost l residues, while B independently and simultaneously acts on the rightmost l residues. In particular, this operation is not commutative: $A \oplus B \neq B \oplus A$, however it is associative, $A \oplus (B \oplus C) = (A \oplus B) \oplus C$. Formally, $(A \oplus B)_{ps,qt} = A_{p,q}\delta_{s,t} + B_{s,t}\delta_{p,q}$, where $\delta_{\sigma,\tau} = 1$ if $\sigma = \tau$ and 0 otherwise. For example, $(A \oplus B)_{ps,qt} = 0$ for $p \neq q$ and $s \neq t$, since the rate for two independent mutations to occur simultaneously vanishes. (Note that this matrix concatenation sum is distinct from the direct sum of matrices, for which the same symbol $\oplus$ is commonly used.) Finally, let O_k be the null matrix on $\mathcal{D}_k$, then the rate matrix for the dinucleotide model on a sequence of length L is

$$\mathcal{R} := \mathcal{R}_L = \sum_{k=1}^{L-1} O_{k-1} \oplus M \oplus O_{L-k-1}. \quad (1)$$

Stationary sequence distribution

The dinucleotide substitution model introduces dependencies between neighbouring sites, and the stationary sequence distribution $\pi(\sigma)$ no longer factorises into a product of single-nucleotide distributions as in the independent-site model. For a certain class of reversible dinucleotide substitution models, the stationary distribution is of Gibbs form (see Pedersen and Jensen (2001)). It can be shown that this implies a (first order) Markov structure for the stationary distribution, that is,

$$p(\sigma_i = \alpha|\sigma_1\sigma_2\cdots\sigma_{i-1}) = p(\sigma_i = \alpha|\sigma_{i-1}) \quad (2)$$

In the general, non-reversible case, numerical experiments seem to indicate that this Markov property breaks down, even though the rate matrix involves only pairwise interactions. It is unclear whether this is a result of the irreversibility of the process, or whether reversibility and having a Markovian stationary distribution are orthogonal features. At any rate, there seems to be no simple expression for the stationary distribution, and we have to resort to a numerical approximation.

The matrix $\mathcal{R}_K$ can be built explicitly for small K, and we can find its stationary distribution numerically by solving $\pi\mathcal{R}_K = 0$. However, this will not properly approximate the marginal distribution $\pi(\sigma_i\cdots\sigma_{i+K-1})$ for a length-K subsequence in a longer sequence of length L, because no substitutions overlapping the edges are taken into account. Such edge effects can be taken into account as follows. First, we note that although (2) is not satisfied exactly, a higher-order Markov property does hold approximately:

$$p(\sigma_i = \alpha|\sigma_1\sigma_2\cdots\sigma_{i-1}) \approx p(\sigma_i = \alpha|\sigma_{i-n}\cdots\sigma_{i-1}), \quad (3)$$

and the approximation converges exponentially in n. If we know the exact marginal distribution π of length-K subsequences, we can use (3) to find the approximate conditional distribution of σ_{K+1},

$$
\begin{aligned}
p(\sigma_{K+1}|\sigma_1\cdots\sigma_K) &\approx p(\sigma_{K+1}|\sigma_2\cdots\sigma_K) \\
&= \frac{\pi(\sigma_2\cdots\sigma_{K+1})}{\sum_{\alpha\in\Omega} \pi(\sigma_2\cdots\sigma_K\alpha)}. \quad (4)
\end{aligned}
$$

This approximation is known as the "K-cluster approximation" in the physics literature (see Arndt et al. (2003); ben Avraham and Köhler (1992)). We can now include edge effects by having the rate matrix M act on $\sigma_K\sigma_{K+1}$ by supposing that σ_{K+1} is distributed according to (4), and similarly for the left-hand edge. Formally, we add to $\mathcal{R}_K$ the rate matrix $\mathcal{R}_K^e$, describing the substitutions at the edges:

$$
\begin{aligned}
(\mathcal{R}_K^e)_{\sigma,\tau} = \Bigg[&\frac{\sum_{\alpha,\beta} \pi(\alpha\sigma_1\cdots\sigma_{K-1})M_{\alpha\sigma_1,\beta\tau_1}}{\sum_\alpha \pi(\alpha\sigma_1\cdots\sigma_{K-1})}\delta_{\sigma[2,K],\tau[2,K]} \\
&+ \frac{\sum_{\alpha,\beta} \pi(\sigma_2\cdots\sigma_K\alpha)M_{\sigma_K\alpha,\tau_K\beta}}{\sum_\alpha \pi(\sigma_2\cdots\sigma_K\alpha)}\delta_{\sigma[1,K-1],\tau[1,K-1]}\Bigg]_{\sigma,\tau}, \\
&\hspace{10cm} (5)
\end{aligned}
$$

where σ and τ are sequences in Ω^K. From an initial guess for π, we compute $\mathcal{R}_K^e$, and then solve $\pi(\mathcal{R}_K + \mathcal{R}_K^e) = 0$ for π to get a better approximation. This procedure is repeated until convergence, which is rapid. The only approximation is made in (4), and since the correlation between nucleotides decreases exponentially fast with their separation, this approximation can be good even for moderate values of K. In this paper, we use $K = 3$.

A recursion for sequence-to-sequence probabilities

Let $v(t)$ be the probability distribution vector at time t, so that $v(t)_\sigma$ is the probability of observing sequence σ at time t. Since the rate at which sequence σ mutates into sequence τ is $\mathcal{R}_{\sigma,\tau}$, the time evolution of v is given by $\mathrm{d}v(t)/\mathrm{d}t = v(t)\mathcal{R}$. The solution to this equation is $v(t) = v(0)\exp(\mathcal{R}t)$, and the probability of sequence σ evolving into τ in time t is $\exp(\mathcal{R}t)_{\sigma,\tau}$. However, the matrix $\mathcal{R}$ is of dimension 4^L, too big for explicit computations. Write $R_i := O_{i-1} \oplus M \oplus O_{L-i-1}$, and recall that $\mathcal{R} = \sum_{i=1}^{L-1} R_i$. We may expand the matrix exponential in a Taylor series,

$$\exp(\mathcal{R}t) = I + \left(\sum_{i=1}^{L-1} R_i\right)\frac{t}{1!} + \left(\sum_{i=1}^{L-1} R_i\right)^2\frac{t^2}{2!} + \cdots \quad (6)$$

Many of the terms in the expression $\left(\sum R_i\right)^n$ commute; indeed, $R_iR_j = R_jR_i$ unless $|i - j| = 1$. We say that a factor $R_{i_1}\cdots R_{i_k}$ is *overlapping* if it cannot be written as the product of two commuting factors. For instance, $R_1R_3R_2$ is overlapping, but $R_1R_4R_2R_5$ is not, since by swapping the middle two factors (which commute), we get $(R_1R_2)(R_4R_5)$, a product of two commuting factors. In this way, a term can be written uniquely as a product of commuting factors, which

themselves are overlapping. We define the *length* of an overlapping factor to be the number of sites it affects; e.g. the length of $R_1 R_2$ is 3 as it affects sites 1 through 3.

Now if a pair of neighbouring sites has never experienced a substitution involving both nucleotides simultaneously, the evolutionary histories of the left and right sequence parts become independent, and the likelihood factorises into a product. If we expand the full likelihood in terms of the first position (counted from the right) where such a 'break' in the dependency structure occurred, we obtain a dynamic programming recursion.

Mathematically, we factorise the terms of (6) into commuting factors. Consider all terms that contain in their factorisation an overlapping factor $F = R_{i_1} \cdots R_{i_n}$ of length k that includes a factor R_{L-1}. The sum of those terms can be written as GF, and this product commutes by construction; F only contains terms R_i with $i > L - k$, whereas G only contains $i < L - k$ terms. In fact, we have

$$
G = I_{L-k} \frac{t^n}{n!} + \left(\sum_{i=1}^{L-k-1} R_i \right) \frac{\binom{n+1}{1} t^{n+1}}{(n+1)!} + \cdots
$$

$$
= \frac{t^n}{n!} \left[I_{L-k} + \left(\sum_{i=1}^{L-k-1} R_i \right) \frac{t}{1!} + \left(\sum_{i=1}^{L-k-1} R_i \right)^2 \frac{t^2}{2!} + \cdots \right]
$$

$$
= \frac{t^n}{n!} \exp\left[(\mathcal{R}_{L-k} \oplus O_k) t \right] = \frac{t^n}{n!} \exp(\mathcal{R}_{L-k} t) \otimes I_k, \quad (7)
$$

where the binomial coefficients $\binom{n+k}{k}$ count the number of ways that k factors R_i can be interleaved with the n factors comprising F in the product $\left(\sum R_i \right)^{n+k}$. Here we introduced the *matrix concatenation product*, $\otimes$, which is defined by $(A \otimes B)_{ps,qt} = A_{p,q} B_{s,t}$, and the symbol I_k denotes the identity matrix on $\mathcal{D}_k$. Recall that $\mathcal{R}_k$ is the rate matrix acting on $\mathcal{D}_k$ as defined in (1). If we denote by A_k the sum of all overlapping factors F of length k, including a factor $\frac{t^n}{n!}$ each, then from (7) if follows that

$$
\exp(\mathcal{R}_n t) = e^{\mathcal{R}_{n-1} t} \otimes A_1 + e^{\mathcal{R}_{n-2} t} \otimes A_2 + \cdots + A_n. \quad (8)
$$

(Here we included the identity matrix I_1 into A_1.) Now let P_n be the probability that the length-n prefix of σ evolves into the same prefix of τ. More formally, $P_n = [\exp(\mathcal{R}_n t)]_{\sigma[1,n], \tau[1,n]}$, where we introduced the notation $\sigma[i,j] = \sigma_i \sigma_{i+1} \cdots \sigma_j$. Then we can turn (8) into the following dynamic programming recursion:

$$
\begin{aligned}
P_n &= (A_1)_{\sigma_n, \tau_n} P_{n-1} + (A_2)_{\sigma[n-1,n], \tau[n-1,n]} P_{n-2} \\
&\quad + (A_3)_{\sigma[n-2,n], \tau[n-2,n]} P_{n-3} + \cdots, \quad (9)
\end{aligned}
$$

with the initialisation $P_0 = 1$. To compute the A_k, we iteratively solve for $A_1, A_2, \ldots$ in (8). For $n = 1$, the equation reads $\exp(\mathcal{R}_1 t) = A_1$, and there is nothing to solve. Note that $\mathcal{R}_1 = 0$ by definition (1), so that $A_1 = I_1$. The other factors

are found recursively:

$$
A_2 = e^{\mathcal{R}_2 t} - e^{\mathcal{R}_1 t} \otimes A_1 \quad (10)
$$

$$
A_3 = e^{\mathcal{R}_3 t} - e^{\mathcal{R}_2 t} \otimes A_1 - e^{\mathcal{R}_1 t} \otimes A_2 \quad (11)
$$

$$
A_4 = e^{\mathcal{R}_4 t} - e^{\mathcal{R}_3 t} \otimes A_1 - e^{\mathcal{R}_2 t} \otimes A_2 - e^{\mathcal{R}_1 t} \otimes A_3 \quad (12)
$$

If these formulas are expanded in terms of the A_k, we get

$$
A_2 = e^{\mathcal{R}_2 t} - A_1 \otimes A_1 \quad (13)
$$

$$
A_3 = e^{\mathcal{R}_3 t} - A_2 \otimes A_1 - A_1 \otimes A_2 - A_1 \otimes A_1 \otimes A_1 \quad (14)
$$

$$
\begin{aligned}
A_4 = \ &e^{\mathcal{R}_4 t} - A_3 \otimes A_1 - A_2 \otimes A_2 - A_1 \otimes A_3 \\
&- A_2 \otimes A_1 \otimes A_1 - A_1 \otimes A_2 \otimes A_1 \\
&- A_1 \otimes A_1 \otimes A_2 - A_1 \otimes A_1 \otimes A_1 \otimes A_1. \quad (15)
\end{aligned}
$$

Collected on the right-hand sides are all possible ways in which a matrix on $\mathcal{D}_k$ can be built from a matrix concatenation product of matrices A_i, $i < k$. By definition, the terms occurring in such products are not overlapping. Since the A_i contain all overlapping terms of length i in the expansion of $\exp(\mathcal{R}_i t)$, the terms in A_k are those in $\exp(\mathcal{R}_k t)$ except terms that factorise, i.e. all overlapping terms of length k.

The recursion (9) is exact, but in practise only a few terms can be included, since the dimension of the matrices A_i grows exponentially with i. Fortunately, the matrix entries tend to 0 exponentially fast, and a good approximation can be obtained with a few terms. In the implementation, we used the Padé algorithm to compute the matrix exponentials of the non-symmetric matrices, see Moler and van Loan (2003).

Evolution from a common ancestor

The algorithm developed above computes the likelihood that one sequence evolves into another. Most often however, we are interested in the likelihood $\mathcal{P}_{\sigma, \tau}$ that two sequences σ and τ have evolved from a common, unknown ancestral sequence ρ. To do this, we compute the exponential of the matrix $\mathcal{R}$ for both branches of the tree using ideas of the previous section, and derive a recursion similar to Felsenstein's reverse traversal algorithm to sum over the ancestral nucleotide distribution. In contrast to Felsenstein's algorithm we cannot immediately carry out this summation, since the equilibrium nucleotide distribution has dependencies along the sequence. Instead, we compute the likelihood conditional on the last few ancestral nucleotide positions, and sum over the ancestral distribution conditional on these. This method can be extended to arbitrary trees, but for simplicity we only give the recursion for the case of a two-leaved tree. Also, we truncate the formulas for the approximation up to the third term, and we use the 3-cluster approximation for the equilibrium distribution. These three-site approximations turn out to be sufficient for our application.

The recursion is, again, conditioned on the shortest sequence suffix that is independent of its prefix, but we now

require this independence to hold on both branches simultaneously. Let $P_n^{\beta\alpha}$ be the likelihood of the descendant sequence prefixes $\sigma[1,n]$ and $\tau[1,n]$ to have evolved from a common ancestral sequence prefix $\rho[1,n]$ in time t_1, t_2 respectively, where the unobserved ancestral sequence is distributed according to the equilibrium distribution, conditional on the last two nucleotides $\rho_{n-1}\rho_n$ being $\beta\alpha$. Analogous to (9) we then have the following dynamic programming recursion:

$$
\begin{aligned}
P_n^{\beta\alpha} = & \sum_\gamma P_{n-1}^{\gamma\beta} p(\gamma|\beta\alpha) B_{\sigma_n,\tau_n}^\alpha \\
& + \sum_{\delta\gamma} P_{n-2}^{\delta\gamma} p(\gamma|\beta\alpha) p(\delta|\gamma\beta) B_{\sigma[n-1,n],\tau[n-1,n]}^{\beta\alpha} \\
& + \sum_{\epsilon\delta\gamma} P_{n-3}^{\epsilon\delta} p(\gamma|\beta\alpha) p(\delta|\gamma\beta) p(\epsilon|\delta\gamma) B_{\sigma[n-2,n],\tau[n-2,n]}^{\gamma\beta\alpha} .
\end{aligned}
$$

(16)

Here $p(\gamma|\beta\alpha) = \pi(\gamma\beta\alpha)/\sum_\delta \pi(\delta\beta\alpha)$ is the probability of observing γ conditional on its right neighbours $\beta\alpha$. This recursion can be made more efficient, removing the double and triple summations, by expressing the stationary distribution in terms of a nucleotide pair further up along the sequence:

$$
\begin{aligned}
P_{n,0}^{\beta\alpha} = & \; P_{n-1,1}^{\beta\alpha} B_{\sigma_n,\tau_n}^\alpha + P_{n-2,2}^{\beta\alpha} B_{\sigma[n-1,n],\tau[n-1,n]}^{\beta\alpha} + \\
& \sum_\gamma P_{n-3,2}^{\gamma\beta} \, p(\gamma|\beta\alpha) B_{\sigma[n-2,n],\tau[n-2,n]}^{\gamma\beta\alpha}
\end{aligned}
$$

(17)

$$
P_{n,k+1}^{\beta\alpha} = \sum_\gamma P_{n,k}^{\gamma\beta} \, p(\gamma|\beta\alpha) \qquad (k=0,1)
$$

(18)

The B-factors represent the probabilities of the events that yield the required dependencies on the two branches, and can be computed by a procedure similar to that used in Sec. :

$$
B_{\sigma_1,\tau_1}^\alpha = (e^{\mathcal{R}_1 t_1})_{\alpha,\sigma_1} (e^{\mathcal{R}_1 t_2})_{\alpha,\tau_1}
$$

(19)

$$
\begin{aligned}
B_{\sigma_1\sigma_2,\tau_1\tau_2}^{\beta\alpha} = & \; (e^{\mathcal{R}_2 t_1})_{\beta\alpha,\sigma_1\sigma_2} (e^{\mathcal{R}_2 t_2})_{\beta\alpha,\tau_1\tau_2} \\
& - B_{\sigma_1,\tau_1}^\beta B_{\sigma_2,\tau_2}^\alpha
\end{aligned}
$$

(20)

$$
\begin{aligned}
B_{\sigma_1\sigma_2\sigma_3,\tau_1\tau_2\tau_3}^{\gamma\beta\alpha} = & \; (e^{\mathcal{R}_3 t_1})_{\gamma\beta\alpha,\sigma_1\sigma_2\sigma_3} (e^{\mathcal{R}_3 t_2})_{\gamma\beta\alpha,\tau_1\tau_2\tau_3} \\
& - B_{\sigma_1,\tau_1}^\gamma B_{\sigma_2\sigma_3,\tau_2\tau_3}^{\beta\alpha} - B_{\sigma_1\sigma_2,\tau_1\tau_2}^{\gamma\beta} B_{\sigma_3,\tau_3}^\alpha - B_{\sigma_1,\tau_1}^\gamma B_{\sigma_2,\tau_2}^\beta B_{\sigma_3,\tau_3}^\alpha
\end{aligned}
$$

(21)

To initialise the recursion, we deviate slightly from the model and assume that the length-L sequence is embedded in an infinitely long sequence. This ensures that the nucleotides at the edges are subjected to the same mutation rates as nucleotides at other positions. This idea is implemented by setting $P_i^{\beta\alpha} = 1$ for $i < 1$, and summing over the unobserved nucleotides σ_i and τ_i with $i < 1$ in (16). At termination, the recursion

(16) is executed for two additional steps, up to $n = L+2$, similarly summing over the unobserved nucleotides σ_i and τ_i with $i > L$. Finally, the likelihood is $\mathcal{P}_{\sigma,\tau} = \sum_{\alpha,\beta} \pi(\beta\alpha) P_{L+2,0}^{\beta\alpha}$.

REFERENCES

Arndt, P. F., Burge, C. B., and Hwa, T. (2003). DNA sequence evolution with neighbor-dependent mutation. *J. Comp. Biol.*, 10(3):313–322.

Averof, M., Rokas, A., Wolfe, K. H., and Sharp, P. M. (2000). Evidence for a high frequency of simultaneous double-nucleotide substitutions. *Science*, 287:1283–1286.

ben Avraham, D. and Köhler, J. (1992). Mean-field (n,m)-cluster approximation for lattice models. *Phys. Rev.*, 45:8358.

E. S. Lander *et al.* (2002). Initial sequencing and comparative analysis of the mouse genome. *Nature*, 420:520 – 562.

Felsenstein, J. (1981). Evolutionary trees from DNA sequences: a maximum likelihood approach. *J. Mol. Evol.*, 17:368–376.

Jensen, J. and Pedersen, A.-M. (2000). Probabilistic models of DNA sequence evolution with context dependent rates of substitution. *Adv. Appl. Prob*, 32:499–517.

Karlin, S. and Burge, C. (1995). Dinucleotide relative abundance extremes: a genomic signature. *Trends in Gen.*, 11(7):283–290.

Moler, C. and van Loan, C. (2003). Nineteen dubious ways to compute the exponential of a matrix, twenty-five years later. *SIAM Review*, 45(1):3–49.

Pedersen, A.-M. and Jensen, J. (2001). A dependent rates model and MCMC based methodology for the maximum likelihood analysis of sequences with overlapping reading frames. *Mol. Biol. Evol*, 18:763–776.

Siepel, A. and Haussler, D. (2003). Combining phylogenetic and hidden Markov models in biosequence analysis. In *Proc. of RECOMB'03*, pages 277–286.

Siepel, A. and Haussler, D. (2004). Phylogenetic estimation of context-dependent substitution rates by maximum likelihood. *Mol. Biol. Evol.*, 21(3):468–488.

Smith, N. G. C., Webster, M. T., and Ellegren, H. (2003). A low rate of simultaneous double-nucleotide mutations in primates. *Mol. Biol. Evol.*, 20(1):47–53.

Subramanian, S. and Kumar, S. (2003). Neutral substitutions occur at a faster rate in exons than in noncoding DNA in primate genomes. *Gen. Res.*, 13(5):838–844.

Sved, J. and Bird, A. P. (1990). The expected equilibrium of the CpG dinucleotide in vertebrate genomes under a mutation model. *Proc. Natl. Acad. Sci. USA*, 87:4692–4696.

von Haeseler, A. and Schöninger, M. (1998). Evolution of DNA of amino acid sequences with dependent sites. *J. Comp. Biol.*, 5(1):149–163.

Whelan, S. and Goldman, N. (2004). Estimating the frequency of events that cause multiple nucleotide changes. *Genetics*. (submitted).

Yang, Z. (1994). Estimating the pattern of nucleotide substitution. *J. Mol. Evol.*, 39:105–111.